Evaluation of CMIP5 Earth System Models for the Spatial Patterns of Biomass and Soil Carbon Turnover Times and Their Linkage with Climate

Donghai Wu, Shilong Piao, Yongwen Liu, Philippe Ciais, Yitong Yao

Evaluation of CMIP5 Earth System Models for the Spatial Patterns of Biomass and Soil Carbon Turnover Times and Their Linkage with Climate

DONGHAI WU, SHILONG PIAO, AND YONGWEN LIU

Sino-French Institute for Earth System Science, College of Urban and Environmental Sciences, Peking University, Beijing, China

PHILIPPE CIAIS

Laboratoire des Sciences du Climat et de l'Environnement, CEA CNRS UVSQ, Gif-sur-Yvette, France

YITONG YAO

Sino-French Institute for Earth System Science, College of Urban and Environmental Sciences, Peking University, Beijing, China

(Manuscript received 5 June 2017, in final form 26 March 2018)

ABSTRACT

Earth system models (ESMs) from phase 5 of the Coupled Model Intercomparison Project (CMIP5) were diagnosed as having large discrepancies in their land carbon turnover times, which partly explains the differences in the future projections of terrestrial carbon storage from the models. Carvalhais et al. focused on evaluation of model-based ecosystem carbon turnover times τ_{eco} in relation with climate factors. In this study, τ_{eco} from models was analyzed separately for biomass and soil carbon pools, and its spatial dependency upon temperature and precipitation was evaluated using observational datasets. The results showed that 8 of 14 models slightly underestimated global biomass carbon turnover times τ_{veg} (modeled median of 8 yr vs observed 11 yr), and 11 models grossly underestimated the soil carbon turnover time τ_{soil} (modeled median of 16 yr vs observed 26 yr). The underestimation of global carbon turnover times in ESMs was mainly due to values for τ_{veg} and τ_{soil} being too low in the high northern latitudes and arid and semiarid regions. In addition, the models did not capture the observed spatial climate sensitivity of carbon turnover time in these regions. Modeled τ_{veg} and τ_{soil} values were generally weakly correlated with climate variables, implying that differences between carbon cycle models primarily originated from structural differences rather than from differences in atmospheric climate models (i.e., related to temperature and precipitation). This study indicates that most models do not reproduce the underlying processes driving regional τ_{veg} and τ_{soil}, highlighting the need for improving the model parameterization and adding key processes such as biotic disturbances and permafrost–carbon climate responses.

1. Introduction

Natural terrestrial ecosystems, excluding those subject to land use change, have sequestered about 30% of cumulative anthropogenic carbon emissions since 2005 (Le Quéré et al. 2015). The global terrestrial carbon sink is sensitive to climate variability and climate trends (Forkel et al. 2016; Peylin et al. 2005; Piao et al. 2013; Xuhui Wang et al. 2014). A positive feedback between the terrestrial carbon reservoir and climate change is projected by Earth system models (ESMs), but the magnitude of this feedback differs among models (Friedlingstein et al. 2014, 2006). How to reduce this uncertainty has received increasing attention recently (Cox et al. 2013).

The carbon turnover time, defined as the ratio of mass and outgoing flux from a carbon pool, is one of the key parameters determining terrestrial carbon balance (He et al. 2016; Koven et al. 2015; Todd-Brown et al. 2013). The structure of land carbon cycle models can be

Supplemental information related to this paper is available at the Journals Online website: https://doi.org/10.1175/JCLI-D-17-0380.s1.

Corresponding author: Shilong Piao, slpiao@pku.edu.cn

DOI: 10.1175/JCLI-D-17-0380.1

summarized by a cascade of pools, each with a different turnover, for different grid points. For example, for live biomass, carbon turnover time in forest is longer than in grasslands; and for dead organic carbon, turnover time in Arctic tundra is much longer than in tropical forests (Bloom et al. 2016). It has been suggested that uncertain carbon turnover time as an emerging property of models dominates the uncertainty in terrestrial vegetation responses to future climate change and rising atmospheric CO_2 concentration (Friend et al. 2014). Furthermore, the soil carbon turnover times in ESMs were shown to be significantly underestimated compared to radiocarbon measurements, leading to overestimation of soil carbon sequestration by a factor of nearly 2 (40% ± 27%) (He et al. 2016).

Terrestrial carbon turnover time is closely linked with climate factors such as temperature and precipitation (Carvalhais et al. 2014; Chen et al. 2013; Knorr et al. 2005). For example, Carvalhais et al. (2014) found a negative correlation between temperature and ecosystem carbon turnover time τ_{eco} across most of the regions in the world, with the exception of tropical forests and warm arid regions. In the warm arid regions, precipitation showed stronger correlations with τ_{eco} than with temperature. In tropical regions, both temperature and precipitation showed a weak spatial correlation with τ_{eco} (Carvalhais et al. 2014). It should be noted that since vegetation and soil carbon turnover have different physiological processes and climate responses (Bradford et al. 2016; De Kauwe et al. 2014), vegetation and soil carbon turnover time may have different spatial patterns of correlation with climate, which was not fully investigated by Carvalhais et al. (2014). Furthermore, it is difficult to draw a clear picture of the terrestrial carbon cycle model performance on the magnitude of the sensitivity of carbon turnover time to climate variation from the current literature.

In addition to the uncertainties in the climate sensitivity of carbon turnover time, the bias of ESM climate fields also influences the modeled carbon turnover times. The simulations from phase 5 of the Coupled Model Intercomparison Project (CMIP5) showed large differences between climate models (Flato et al. 2013). For example, the CMIP5 global land annual temperature T during the period of 1986–2005 differed by approximately 3°C among models, and global land annual precipitation P by approximately 250 mm (Anav et al. 2013). This invites the question whether large differences of turnover times between CMIP5 ESMs mainly result from differences between climate models or from structural differences between carbon cycle models.

In this study, we evaluated the spatial patterns of carbon turnover time and its response to climate variation derived from 14 CMIP5 ESMs against observation-based results. Unlike previous studies such as Carvalhais et al. (2014), here we evaluate biomass and soil carbon turnover time separately. Annual net primary production instead of gross primary production was used to calculate carbon turnover time.

2. Dataset and methods

a. Vegetation carbon storage

The spatial distribution of total biomass carbon was derived from recently published global maps of aboveground biomass carbon (ABC) over the period of 1993–2010 (Liu et al. 2015) and biome-specific conversion factors between total biomass carbon (TBC) and ABC (Flato et al. 2013; Liu et al. 2015; Robinson 2007). The global ABC product of Liu et al. (2015) was derived based on global vegetation optical depth (VOD) retrievals from harmonized series of passive microwave satellite sensors (Liu et al. 2011). Similar to Liu et al. (2015), in order to retrieve the TBC we simply multiplied ABC values by vegetation-specific ratios of TBC/ABC, provided by Table 1 in Liu et al. (2015). The information on the spatial distribution of vegetation type was determined using the Moderate Resolution Imaging Spectroradiometer (MODIS) International Geosphere–Biosphere Program (IGBP) land-cover map (Friedl et al. 2010). Our estimation of the global TBC stock was 570 PgC, comparable to the 560 PgC from Gibbs et al. (2006).

b. Soil organic carbon storage

Previous studies usually used the best traditional soil carbon map provided by the Harmonized World Soil Database (HWSD) (FAO/IIASA/ISRIC/ISSCAS/JRC 2012) and the Northern Circumpolar Soil Carbon Database (NCSCD) (Hugelius et al. 2013; Tarnocai et al. 2009) for estimating soil carbon turnover time (Todd-Brown et al. 2013). In this study, we chose the latest global soil carbon dataset provided by the World Inventory of Soil Emission Potentials (WISE) project (Batjes 2016) based on approximately 21 000 available profiles and soil geographical data. The WISE soil carbon dataset has more accurate spatial patterns of soil organic carbon (SOC) especially for the northern circumpolar regions, and reported SOC density for seven depth intervals (0–0.2, 0.2–0.4, 0.4–0.6, 0.6–0.8, 0.8–1.0, 1.0–1.5, and 1.5–2.0 m). Because the CMIP5 models did not include vertically resolved soil profiles, and did not consider carbon cycle processes for burying carbon below the active layer, we used the top 1 m of soil carbon storage to compute soil carbon turnover time as in Todd-Brown et al. (2013). To compare with modeled results,

we also used the global litter carbon stock from Bloom et al. (2016) output by a diagnostic ecosystem carbon balance model, Data Assimilation Linked Ecosystem Carbon Model version 2 (DALEC2) (Bloom and Williams 2015). In this study, soil organic carbon storage was calculated from the sum of soil carbon from Batjes (2016) and litter carbon from Bloom et al. (2016).

c. NPP and climate data

The global distribution of net primary production (NPP) with 1-km spatial resolution from 2000 to 2010 was provided by the Numerical Terradynamic Simulation Group (NTSG) at the University of Montana (https://www.ntsg.umt.edu/; Zhao and Running 2010). This NPP product was not an observation but a model with a light-use efficiency formulation driven by satellite-based estimates of the fraction of photosynthetically active radiation, shortwave downward solar radiation, vapor pressure deficit (VPD), and low daily minimum temperature for gross primary production (GPP), and a model for maintenance and growth components respirations to derive NPP from GPP. Detailed information on the techniques used for modeling NPP can be found in related publications (Zhao and Running 2010; Zhao et al. 2005).

The temperature and precipitation data were from the Climatic Research Unit (CRU) time series version 3.24 datasets (Harris et al. 2014) with a spatial resolution of 0.5°. These gridded datasets were obtained from more than 4000 meteorological stations and interpolated based on spatial autocorrelation functions (Mitchell and Jones 2005; New et al. 2000).

d. CMIP5 ESM simulations

We used historical simulations (''historical'' experiment, 1850–2005) from the CMIP5 ESMs forced by observed atmospheric composition changes and time-variable land cover (Taylor et al. 2012). Output of biomass carbon, soil organic carbon, litter carbon, NPP, air temperature, and precipitation (cVeg, cSoil, cLitter, npp, tas, and pr in the CMIP5 variable list) from 14 ESMs (see Table S1 in the supplemental information) were used. These monthly output variables were downloaded from the PCMDI server (Cinquini et al. 2014; http://cmip-pcmdi.llnl.gov/cmip5). For models with multiple simulations, all members of the ensemble were averaged following Todd-Brown et al. (2013, 2014). All ESM data were regridded to 1° × 1° spatial resolution using a first-order conservative remapping scheme (Jones 1999) in Climate Data Operators (https://code.zmaw.de/projects/cdo).

e. Analyses

Carbon turnover time is usually defined as the ratio between the mass of a carbon pool and its output flux (Koven et al. 2015). In general, the output flux for biomass corresponds to litter fall (including tree mortality) and fires, while heterotrophic respiration corresponds to the output flux of soil carbon and litter. Because of the lack of observed information on the global distribution of output flux related materials (vegetation litter fall and heterotrophic respiration), here we used the input flux of annual NPP to calculate biomass and soil carbon turnover time [see Eqs. (1) and (2)]:

$$\tau_{\text{veg}} = \frac{C_{\text{veg}}}{\text{NPP}} \quad \text{and} \tag{1}$$

$$\tau_{\text{soil}} = \frac{C_{\text{soil}}}{\text{NPP}}, \tag{2}$$

where τ_{veg} and τ_{soil} refer to the biomass and soil turnover times; C_{veg} and C_{soil} refer to the biomass and soil carbon storage (cSoil + cLitter, from CMIP5). Under the assumption that the difference between carbon input and output in near steady state is small compared to the magnitude of each gross flux, the net primary production and loss from vegetation and heterotrophic respiration from soil are close to each other. The time frame of the variables used in estimating the carbon turnover times was from 2000 to 2005, the common period between satellite-based NPP fluxes and historical simulation results from CMIP5. At the global and biome scales, τ_{veg} and τ_{soil} were derived from the total carbon storage (C_{veg} and C_{soil}) and NPP fluxes.

In Carvalhais et al. (2014), the association between climate variables (temperature and precipitation) and τ_{eco} was determined by analyzing correlation coefficients to identify the dominant climate factors in local ecosystems. In contrast, we are interested here in both the sign and magnitude of the spatial sensitivities of carbon turnover times. Thus, we estimated the local spatial sensitivity (linear regression slope) of τ_{veg} and τ_{soil} to mean annual temperature (MAT) and mean annual precipitation (MAP) in 5° × 5° moving windows around each 1° grid cell, using the following multiple regression:

$$y = \gamma x_T + \delta x_P + c + \varepsilon, \tag{3}$$

where y is τ_{veg} or τ_{soil}; x_T and x_P represent MAT and MAP, respectively; γ and δ define the apparent sensitivities of carbon turnover to spatial gradients in temperature and precipitation, respectively (Piao et al. 2013); c is a constant; and ε is the residual error term. Here ''apparent'' indicates the empirical partial derivative of carbon turnover time to each climate variable, but in reality these factors covary. We tested the statistical significance of γ and δ at the 0.05 level. If model-based spatial sensitivity values of carbon turnover times were beyond the 5th–95th uncertainty

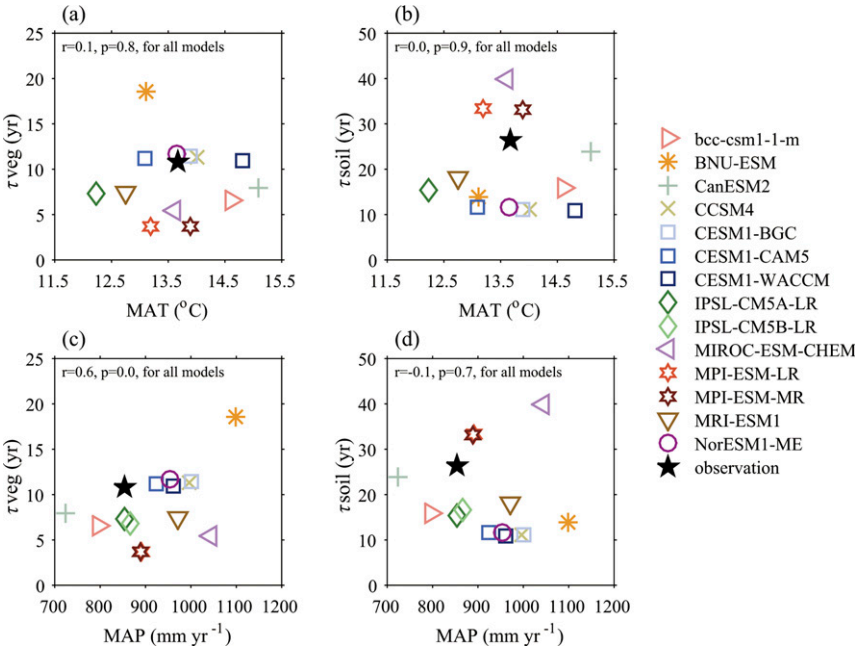

FIG. 1. The magnitude of global MAT and MAP with τ_{veg} and τ_{soil} estimated by 14 CMIP5 ESMs and observational data, (a) MAT and τ_{veg}; (b) MAT and τ_{soil}; (c) MAP and τ_{veg}; and (d) MAP and τ_{soil}. Note that r is the Pearson correlation coefficient between MAT or MAP and τ_{veg} or τ_{soil} for all models; p is the corresponding significance.

range of the observation-based spatial sensitivity, we supposed that the model failed to capture the observation at corresponding regional grids. Furthermore, we have checked the robustness of spatial sensitivity of carbon turnover time to climate in a 7° × 7° moving window, and again in a 9° × 9° moving window.

3. Results

a. Carbon turnover time at the global and biome scale

Compared to observation-based τ_{veg} (~11 yr), 8 of the 14 CMIP5 ESMs [BCC_CSM1.1(m), CanESM2, IPSL-CM5A-LR, IPSL-CM5B-LR, MIROC-ESM-CHEM, MPI-ESM-LR, MPI-ESM-MR, and MRI-ESM1] underestimate τ_{veg}, and 5 ESMs [CCSM4, CESM1(BGC), CESM1 (CAM5), CESM1(WACCM), and NorESM1-ME] have a value comparable to observed (Figs. 1a,c). Among the 14 models, the shortest global τ_{veg} is simulated by MPI-ESM-MR (4 yr), and BNU-ESM predicted the longest τ_{veg} (19 yr), with a factor of 4.8 across the models. As shown in Figs. 1a and 1c, the large differences of τ_{veg} across ESMs are correlated with precipitation ($r = 0.6, p = 0.0$) but not with temperature differences ($r = 0.1, p = 0.8$), implying that the bias of modeled precipitation rather than temperature may explain some of the differences in τ_{veg} at the global scale.

Global τ_{soil} based on the WISE soil dataset is 26 yr (Fig. 1). The 14 CMIP5 ESMs estimated τ_{soil} ranging from 11 yr [CESM1(WACCM)] to 40 yr (MIROC-ESM-CHEM), with a median value of 16 yr, thus grossly underestimating τ_{soil} (even though 3 models—MIROC-ESM-CHEM, MPI-ESM-LR, and MPI-ESM-MR—overestimate τ_{soil}). The model-estimated global τ_{soil} is weakly positively correlated with temperature ($r = 0.0, p = 0.9$) and negatively correlated with precipitation ($r = -0.1, p = 0.7$) across the models (Figs. 1b,d), indicating that the differences of τ_{soil} between models primarily originate from structural differences in terrestrial carbon cycle models rather than from errors in climate models.

For different biomes (see Fig. S1 in the supplemental material), we observed that most models largely underestimated τ_{veg} and τ_{soil} in tundra (modeled median of 7 yr vs observed 12 yr for τ_{veg} and 40 vs 118 yr for τ_{soil}; Fig. 2a) and in desert and shrubland (modeled median of 4 yr vs observed 14 yr for τ_{veg} and 18 vs 54 yr for τ_{soil}; Fig. 2e). In other biomes, model-based carbon turnover times showed large variation, but the median of the models provides similar values to observations for tropical forest (12 vs 14 yr for τ_{veg} and 9 vs 11 yr for τ_{soil}; Fig. 2c) and temperate forest (10 vs 9 yr for τ_{veg} and 17 vs 18 yr for τ_{soil}; Fig. 2d).

b. Spatial distribution of τ_{veg} and τ_{soil}

The carbon turnover times derived from observational data show spatial gradients (Figs. 3a and 4a). Longer τ_{veg} (>20 yr) prevail in boreal forests and arid

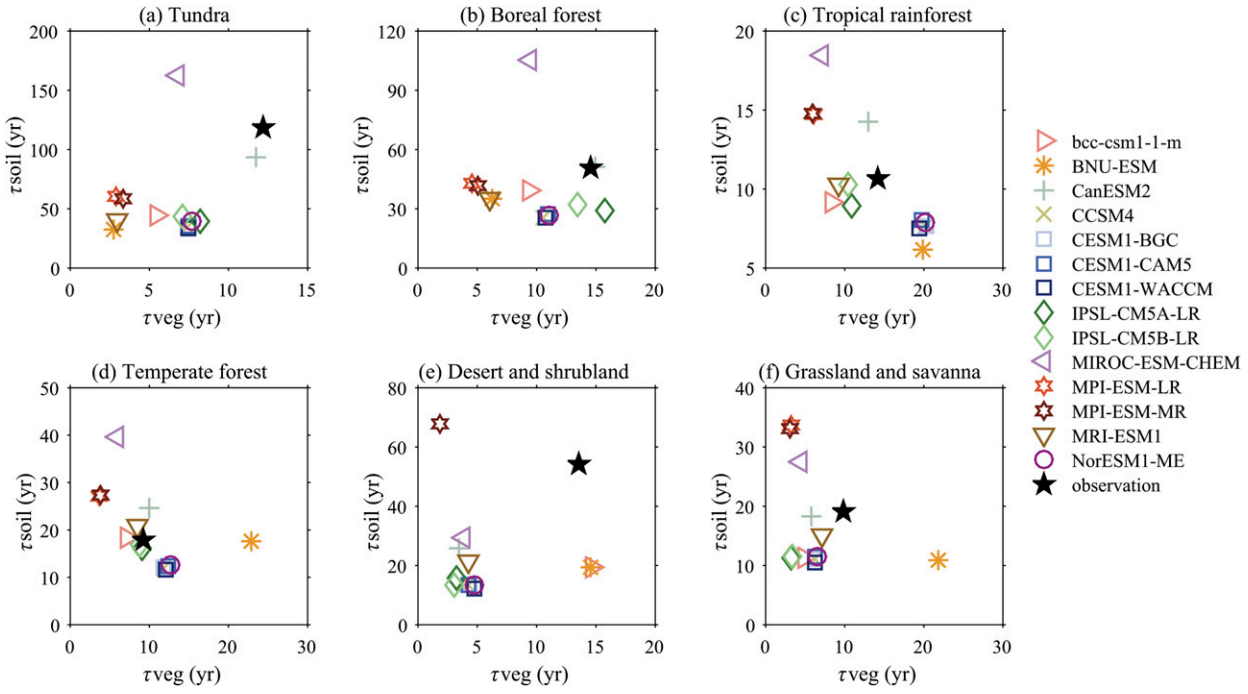

FIG. 2. The magnitude of τ_{veg} vs τ_{soil} of six biomes estimated by 14 CMIP5 ESMs and observational data, for (a) tundra, (b) boreal forest, (c) tropical rain forest, (d) temperate forest, (e) desert and shrubland, and (f) grassland and savanna.

and semiarid regions (western United States, western China, the sub-Saharan region, and central Australia), while temperate cropland-dominated regions (e.g., central North America, eastern Europe, and eastern China) have short τ_{veg} (<4 yr). The τ_{veg} of tropical forests is longer than 12 yr. Similar spatial patterns of τ_{veg} are reproduced by most ESMs (except BNU-ESM and MRI-ESM1; Fig. S2 in the supplemental material), although there are large differences in the spatial gradients of τ_{veg} (Fig. 3). In fact, τ_{veg} is underestimated over more than half the land area ($\Delta\tau_{veg} < -3$ yr, where $\Delta\tau_{veg}$ is the difference between observation-based and model-based τ_{veg}) for 13 out of 14 models (excluding BNU-ESM). The two models with the largest areas of underestimated τ_{veg} are MPI-ESM-LR and MPI-ESM-MR. BNU-ESM has the largest area of mismatch with the observations. It is noticeable that most models underestimate biomass turnover times in arid and semiarid regions as well as in northeastern Siberia, but overestimate τ_{veg} in eastern North America, southern Europe, and eastern China (Fig. 3). Across tropical forested regions, 5 of 14 models [CCSM4, CESM1(BGC), CESM1(CAM5), CESM1(WACCM), and NorESM1-ME] largely overestimate τ_{veg} ($\Delta\tau_{veg} > 5$ yr). Model-based τ_{veg} is weakly correlated with temperature (5.3% land area, $p < 0.05$; Fig. S4) and with precipitation (4.3% land area, $p < 0.05$; Fig. S4) across local climate gradients, confirming that differences of τ_{veg} mainly generate from the coupled land models rather than climate models.

In contrast with τ_{veg} (Fig. 3a), tropical forested area show lowest τ_{soil} (<20 yr). As shown in Fig. 4a, the largest τ_{soil} are mainly in the temperate arid and semiarid regions as well as high-latitude tundra regions, where $\tau_{soil} > 80$ yr. Note that τ_{soil} in most ESMs generally show similar spatial patterns, with the shortest τ_{soil} in tropical forest regions and longest τ_{soil} in the Arctic tundra region (Fig. S3 in the supplemental material). Compared with τ_{soil} derived from observation, 9 out of 14 models [BCC_CSM1.1(m), BNU-ESM, CCSM4, CESM1(BGC), CESM1(CAM5), CESM1(WACCM), IPSL-CM5A-LR, IPSL-CM5B-LR, and NorESM1-ME] systematically underestimate τ_{soil} ($\Delta\tau_{soil} < -5$ yr, where $\Delta\tau_{soil}$ is the difference between observation-based and model-based τ_{soil}), with CCSM4 showing the largest underestimated area. On the contrary, MIROC-ESM-CHEM (Fig. 4k), MPI-ESM-LR (Fig. 4l), and MPI-ESM-MR (Fig. 4m) overestimate τ_{soil} ($\Delta\tau_{soil} > 5$ yr) in about half of the land area. All models largely underestimate τ_{soil} ($\Delta\tau_{soil} < -50$ yr) in arid and semiarid regions across southwestern North America, western China, the sub-Saharan region, and Australia (Figs. 4b–o). In northern high-latitude regions with permafrost, shorter τ_{soil} than observed ($\Delta\tau_{soil} < -10$ yr) is predicted by most models except MIROC-ESM-CHEM, which significantly overestimates τ_{soil} ($\Delta\tau_{soil} > 50$ yr) (Fig. 4k).

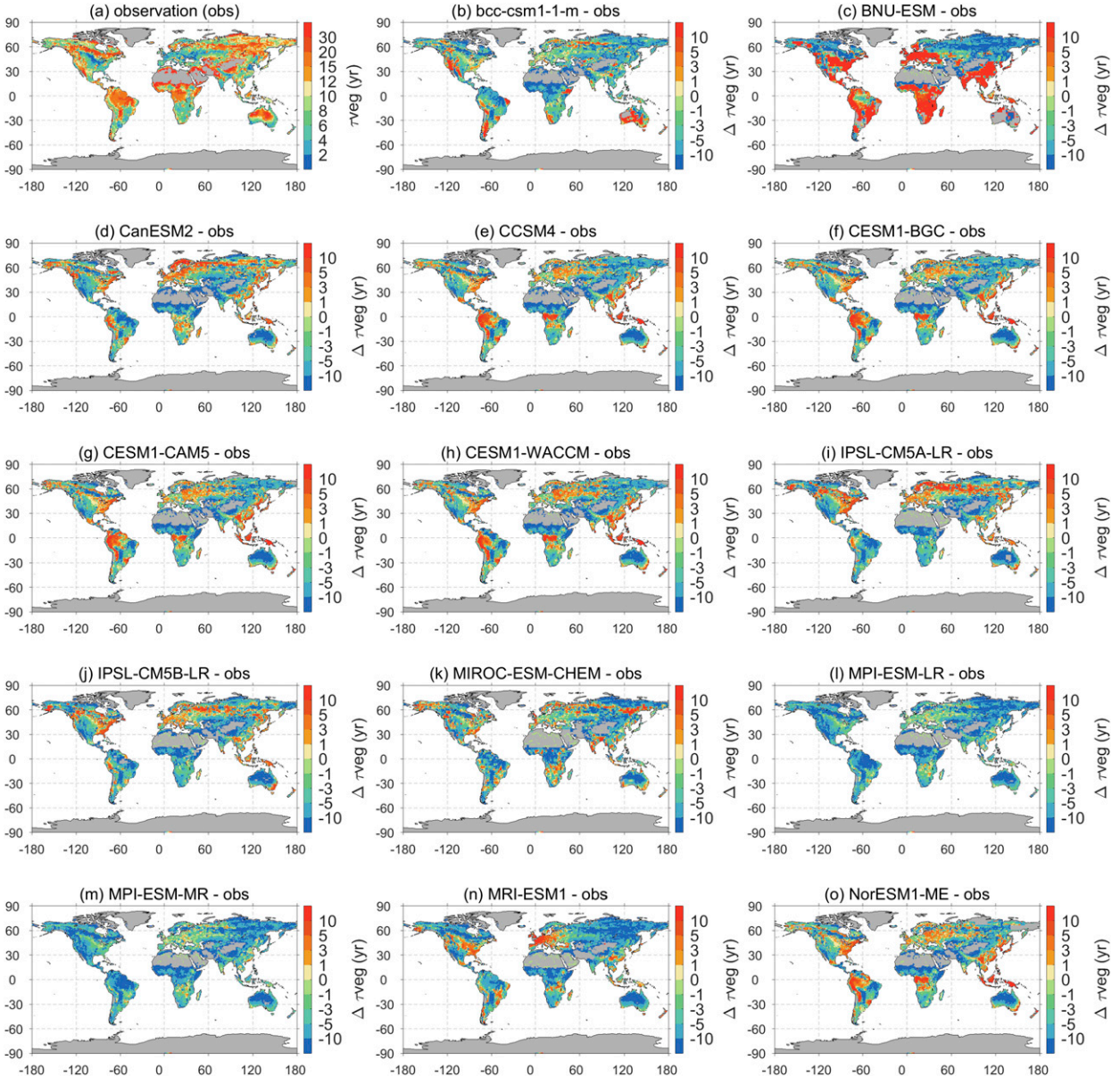

FIG. 3. (a) Global spatial patterns of τ_{veg} derived from observation data (obs) and (b)–(o) observation differences with model-based τ_{veg}. Areas with no biomass (mean annual NDVI below 0.1) are masked with gray shading.

For spatial correlations between model-based τ_{soil} and climate, there is only a small area showing significant values at the $p < 0.05$ level for τ_{soil} and temperature (6.2% land area; Fig. S4) and for τ_{soil} and precipitation (5.3% land area; Fig. S4).

As shown in Fig. 5a, model-based τ_{soil} show higher spatial correlation with observation than τ_{veg} (correlation coefficients with τ_{soil} generally larger than 0.4 except for BNU-ESM, and correlation coefficients smaller than 0.3 for all models for τ_{veg}), implying that ESMs have better performance in the simulation of spatial patterns of τ_{soil} than τ_{veg}. Overall, among the 14 models, MIROC-ESM-CHEM shows the highest spatial correlation of τ_{soil} with the observation ($r = 0.7$), while NorESM1-ME has the highest spatial correlation of τ_{veg} with the observation ($r = 0.3$). In terms of root-mean-square error (RMSE) between the observation and simulations across the globe (Fig. 5b), we found that NorESM1-ME and MPI-ESM-LR show the lowest RMSE for τ_{veg} (8 yr) and τ_{soil} (38 yr), respectively. The highest RMSE appears in BNU-ESM for both τ_{veg} (36 yr) and τ_{soil} (77 yr).

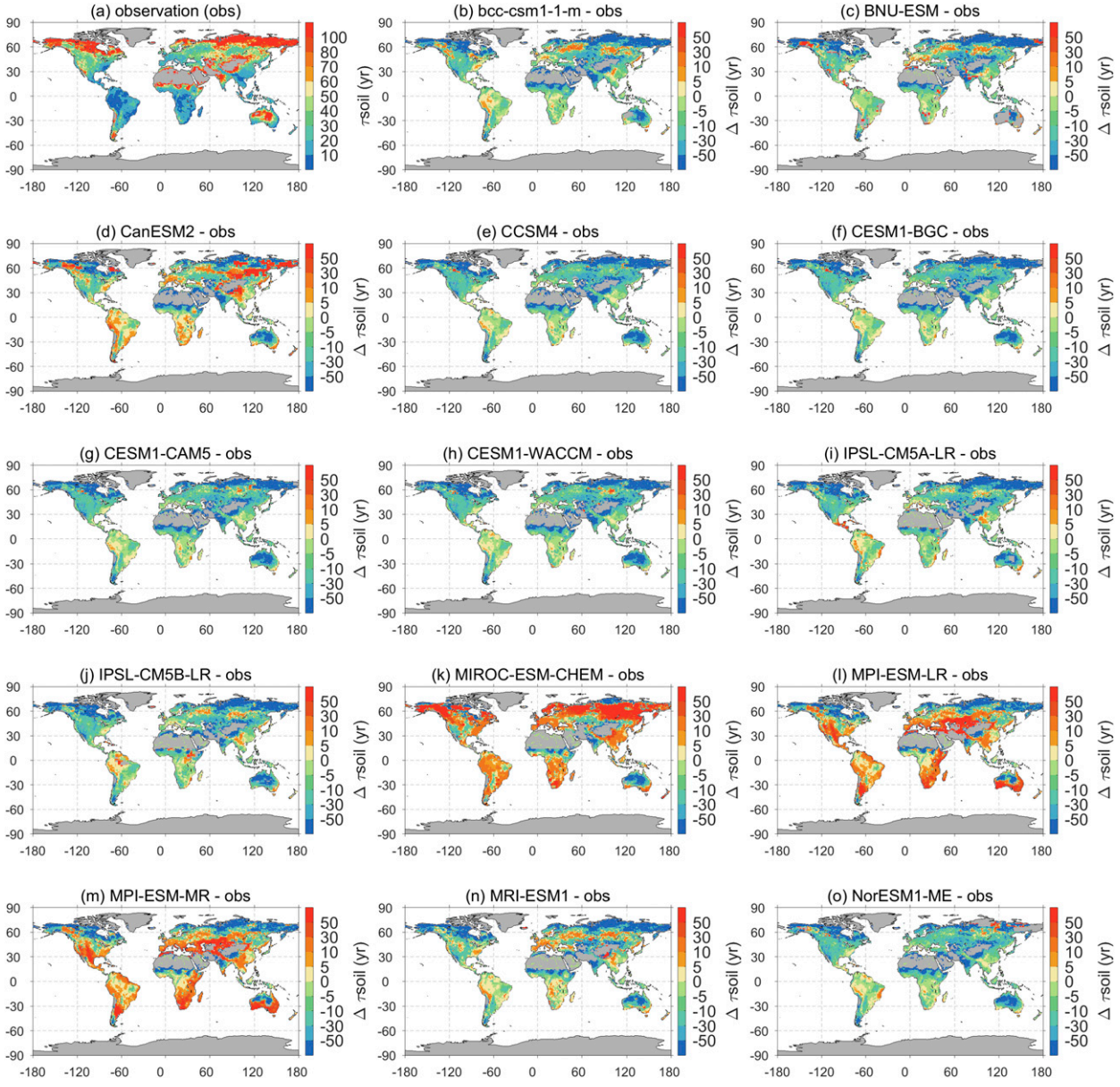

FIG. 4. As in Fig. 3, but for τ_{soil}.

c. *Spatial sensitivities of carbon turnover times to climate*

To further study the spatial sensitivities of τ_{veg} and τ_{soil} to climate (temperature and precipitation), we performed multiple linear regression analysis as explained in the method section. As shown in Fig. 6a, the observation-based sensitivities of τ_{veg} to temperature (denoted as $\gamma_T^{\tau veg}$) varied across different regions, with 95% confidence interval values in the range from -4 to approximately $5\,yr\,°C^{-1}$. Significant negative $\gamma_T^{\tau veg}$ ($<-1\,yr\,°C^{-1}$) are generally observed across boreal forests and tundra of northern Siberia, indicating faster biomass carbon turnover with increasing temperature. In contrast, tropical forests (except South Asia) and drylands in Australia show significant positive $\gamma_T^{\tau veg}$ ($>1\,yr\,°C^{-1}$). The sign of $\gamma_T^{\tau veg}$ estimated by most ESMs is opposite to observations in the Amazon forest and in the tundra region of northern Siberia. Although most ESMs (except BNU-ESM) correctly capture the sign of $\gamma_T^{\tau veg}$ in other regions, the magnitude of model-based $\gamma_T^{\tau veg}$ is also lower than that of observation (Figs. 6a,c and Fig. S5 in the supplemental material).

Observation-based precipitation sensitivities of τ_{veg} (denoted as $\delta_P^{\tau veg}$) also show large spatial heterogeneity

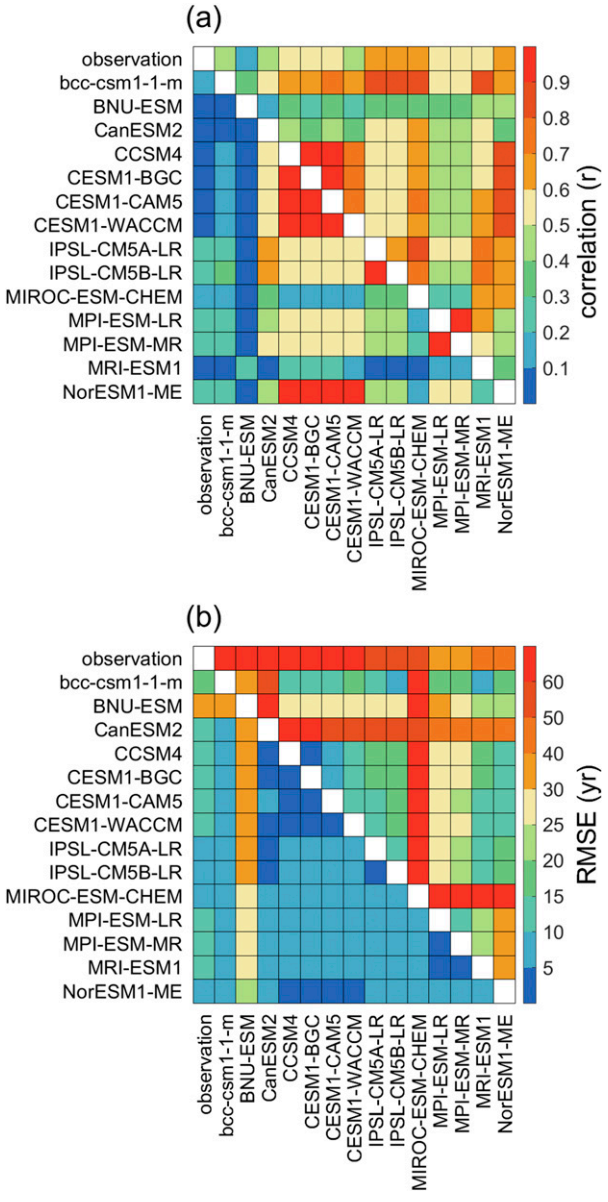

FIG. 5. Matrices of (a) r and (b) RMSE for carbon turnover times between each CMIP5 ESM and observation and between CMIP5 ESMs at the grid cells. Lower-triangular matrix represents r or RMSE for τ_{veg}, and upper-triangular matrix represents r or RMSE for τ_{soil}.

(Fig. 6b). Across boreal and Arctic regions, observation-based sensitivities to precipitation are positive $\delta_P^{\tau veg}$ [>5 yr $(100\,mm)^{-1}$]. This longer τ_{veg} with increasing precipitation is correctly represented by several ESMs including BCC_CSM1.1(m), CanESM2, CCSM4, CESM1(BGC), CESM1(CAM5), CESM1(WACCM), and MIROC-ESM-CHEM (Fig. S6). In contrast, relative large negative values $\delta_P^{\tau veg}$ [<-5 yr $(100\,mm)^{-1}$] are found in arid and semiarid regions (central Asia, the sub-Saharan region, and northern Australia) where 13 of 14 models [except BCC_CSM1.1(m), which overestimates $\delta_P^{\tau veg}$ in Australia] show opposite sensitivities of τ_{veg} to precipitation compared to observation-based values (Figs. 6b,d and Fig. S6 in the supplemental material).

Figure 7 shows the spatial sensitivities of observation-based τ_{soil} to temperature (denoted as $\gamma_T^{\tau soil}$) and precipitation (denoted as $\delta_P^{\tau soil}$). Similar to the spatial patterns of observed $\gamma_T^{\tau veg}$ (Fig. 6a), τ_{soil} generally decreases with increasing temperature across spatial climate gradients (with values $<-5\,yr\,°C^{-1}$) in boreal and Arctic regions, but the sensitivities to temperature are positive in tropical forests (except South Asia) and drylands, such as in Australia ($>5\,yr\,°C^{-1}$) (Fig. 7a). As shown in Fig. 7c and Fig. S7 in the supplemental material, most ESMs perform better in simulating $\gamma_T^{\tau soil}$ over boreal and arctic regions than over tropical regions. For example, 12 of 14 models (except BNU-ESM and MRI-ESM1) also show negative values of $\gamma_T^{\tau soil}$ across boreal and Arctic regions, while only one model (IPSL-CM5B-LR) captured parts of the observation-based dramatic positive $\gamma_T^{\tau soil}$ in tropical regions.

In terms of $\delta_P^{\tau soil}$, a relatively weak sensitivity is observed in tropical regions (Fig. 7b), consistent with most ESMs (Fig. 7d and Fig. S8 in the supplemental material). In temperate arid and semiarid regions, a negative $\delta_P^{\tau soil}$ is observed with the highest sensitivity lower than -10 yr $(100\,mm)^{-1}$. Although most of ESMs also predict negative $\delta_P^{\tau soil}$ in these regions, they underestimate the magnitude of the negative sensitivity (Figs. 7d and S8). A heterogeneous distribution of $\delta_P^{\tau soil}$ is observed in boreal and Arctic regions (Fig. 7b), and there is a poor agreement between observation and ESMs.

Furthermore, we have conducted spatial sensitivity of carbon turnover time to climate in a 7° × 7° moving window (Figs. S9 and S10 in the supplemental material) and in a 9° × 9° moving window (Figs. S11 and S12). In results, most of the spatial patterns are similar based on the three moving window methods, which emphasizes the robustness of the spatial sensitivities of carbon turnover time to climate. Here, we chose the results based on the 5° × 5° moving window, similar to Carvalhais et al. (2014), because larger moving windows, containing more nonuniform biome types and environmental factors, would induce greater uncertainties, especially for the transitional zones of different vegetation types.

4. Discussion

a. Observed global carbon turnover time

Compared to the previous study (τ_{veg} = 4 yr based on GPP) of Carvalhais et al. (2014), a much longer global τ_{veg} (11 yr) is obtained in this study. This difference is

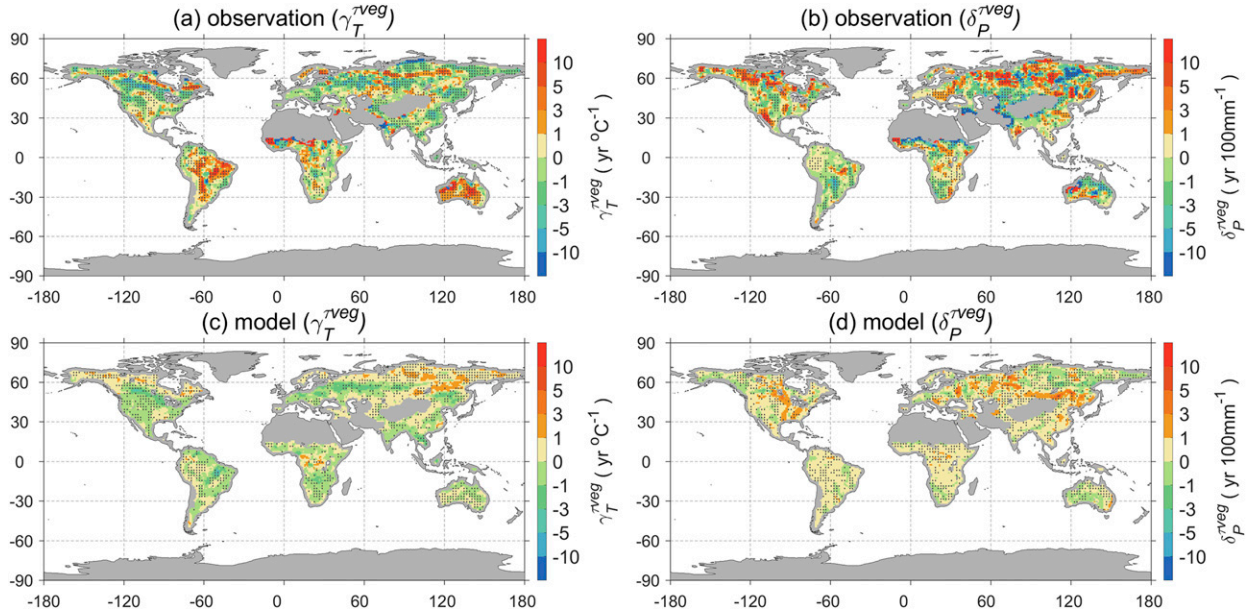

FIG. 6. Spatial sensitivity of $\gamma_T^{\tau veg}$ and $\delta_P^{\tau veg}$ in a 5° × 5° moving window using a multiple linear regression approach, sensitivity of observation-based (a) $\gamma_T^{\tau veg}$ and (b) $\delta_P^{\tau veg}$ and median sensitivity of model-based (c) $\gamma_T^{\tau veg}$ and (d) $\delta_P^{\tau veg}$. For example, positive $\gamma_T^{\tau veg}$ suggests that warmer temperature is associated with longer τ_{veg}, and the value represents the change of τ_{veg} with a temperature gradient of 1°C. In (a) and (b), stippling indicates locations where observation-based sensitivity is significant ($p < 0.05$); in (c) and (d), stippling indicates where fewer than one-quarter of the models are within the 5th–95th uncertainty range of the observed sensitivity. Areas with no biomass (mean annual NDVI below 0.1) are masked with gray shading.

mainly due to the different definition of τ_{veg} as we used NPP instead of GPP. NPP is arguably more relevant for the fate of carbon being removed from the atmosphere on time scales longer than a year and stored into terrestrial pools. In contrast to τ_{veg}, our estimation of the global value of τ_{soil} (26 yr) is much smaller than derived by Carvalhais et al. (2014) (46 yr). This is because Carvalhais et al. (2014) estimated τ_{soil} using total soil stocks for full depth, while we used soil stocks for 1-m depth. As mentioned in section 2, the main purpose of this study is to evaluate ESMs estimated carbon turnover time, and the CMIP5 ESMs did not consider processes to burying carbon below the active layer (Tian et al. 2015; Todd-Brown et al. 2013). Our estimates are in consistent with the global τ_{veg} of 10 yr in Jiang et al. (2015) and with the global τ_{soil} of 24 yr in Todd-Brown et al. (2013).

b. *Comparison of observed and ESMs estimated carbon turnover time*

Compared with observations, ESMs generally underestimate τ_{veg}, particularly in the high northern latitudes and arid and semiarid regions (Fig. 3), where models also do not capture the observation-based spatial climate sensitivity of τ_{veg} (Fig. 6). The spatial $\gamma_T^{\tau veg}$ estimated from observations indicate a decrease of τ_{veg} in response to higher temperature in the northern high latitudes, while models produce a sensitivity of opposite sign, particularly in northern Siberia. It has been suggested that drought driven by increases in temperature enhance fire risks and insect attacks (Raffa et al. 2008; Williams et al. 2010, 2013), which increase mortality rate and accelerate biomass carbon turnover (Allen et al. 2010; Van Mantgem and Stephenson 2007). However, climate-induced mortality and biotic disturbances are largely ignored in current ecosystem models (Anderegg et al. 2015; Thurner et al. 2016, 2017). In addition to drought-induced increase in tree mortality, most ESMs do not consider carbon–nitrogen interactions, which may also indirectly explain the opposite temperature sensitivity of τ_{veg} between observation and ESMs in boreal regions (Friedlingstein et al. 2014; Piao et al. 2013). Northern ecosystems are generally limited by low temperature and nitrogen (Janssens et al. 2010; Melillo et al. 2002; Nemani et al. 2003). Higher temperature enhance nitrogen mineralization, and thus increase in soil nitrogen availability for vegetation carbon assimilation and biomass growth (Melillo et al. 2002). The enhanced nitrogen availability also leads to more NPP allocated in parts of aboveground biomass (e.g., foliar and wood) (Greaver et al. 2016; Janssens et al. 2010), which may eventually result in faster plant metabolism (Niu et al. 2010), also accompanied by vulnerability to attack (e.g., wind,

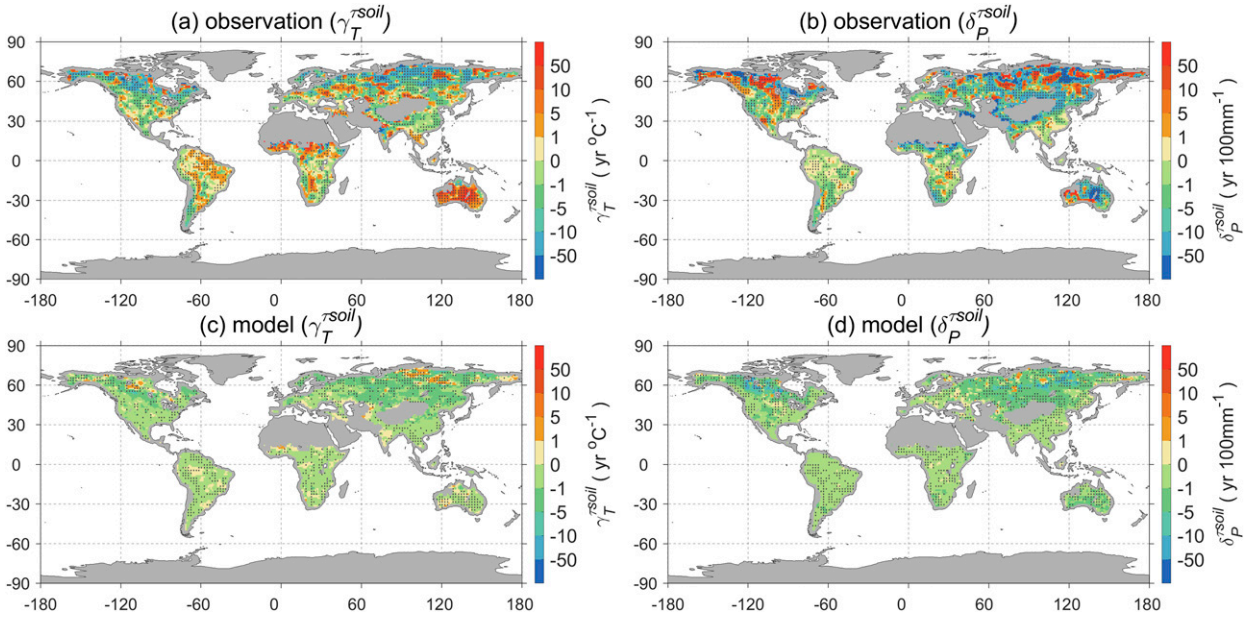

FIG. 7. Spatial sensitivity of $\gamma_T^{\tau soil}$ and $\delta_P^{\tau soil}$ in a 5° × 5° moving window using a multiple linear regression approach, sensitivity of observation-based (a) $\gamma_T^{\tau soil}$ and (b) $\delta_P^{\tau soil}$ and median sensitivity of model-based (c) $\gamma_T^{\tau soil}$ and (d) $\delta_P^{\tau soil}$. For example, positive $\delta_P^{\tau soil}$ suggests that increasing precipitation is associated with longer τ_{soil}, and the value represents the change of τ_{soil} with a precipitation gradient of 100 mm. In (a) and (b), stippling indicates locations where observation-based sensitivity is significant ($p < 0.05$); in (c) and (d), stippling indicates where fewer than one-quarter of the models are within the 5th–95th uncertainty range of the observed sensitivity. Areas with no biomass (mean annual NDVI below 0.1) and data are masked with gray shading.

insects, and pathogens) (Franklin et al. 1987; Stephenson et al. 2011). All these causes may increase the forest mortality rates, suggesting a negative apparent climatic $\gamma_T^{\tau veg}$. In contrast to boreal regions, growing season temperature is close to a high temperature threshold of vegetation growth in tropical forests (Corlett 2011; Piao et al. 2013). Accordingly, regions with higher temperature generally have lower vegetation productivity (Doughty and Goulden 2008; Tribuzy 2005). It has been also suggested that tree mortality rates are positively correlated with forest NPP through many mechanisms including trade-offs between growth and defense and between reproduction and persistence (Stephenson et al. 2011). These ecological processes may induce positive $\gamma_T^{\tau veg}$ in tropical forests.

Similar to τ_{veg}, ESMs generally underestimate the τ_{soil}. As shown in Fig. 4, 13 out of 14 models predicted shorter τ_{soil} in the northern high latitudes with permafrost, compared with observation. This may be related to the fact that permafrost processes were not taken into account in the CMIP5 ESMs (Burke et al. 2013; Schuur et al. 2015). Permafrost soil contains large amounts of organic carbon, which would be vulnerable with higher decomposition rates under rapid global warming (Koven et al. 2011). Combined reductions in the thawed season length and thawed soil depth during the warm season in these cold regions compared to warm climates could results in higher $\gamma_T^{\tau soil}$ (Koven et al. 2017). However, most models used a fixed quotient of change in respiration caused by change in temperature by 10°C (Q_{10}) and a single layer with soil decomposition closely related to near-surface temperature, which fail to capture the soil freeze–thaw processes affecting decomposition rates and underestimate the apparent τ_{soil} (Koven et al. 2017; Wieder et al. 2018). In contrast to high latitudes, a positive value of $\gamma_T^{\tau soil}$ is generally observed in arid and semiarid regions including southwestern China, western Asia, western North America, and Australia. This is because lower soil moisture associated with temperature limits soil organic carbon decomposition (Xin Wang et al. 2014). Indeed, a negative value of $\delta_P^{\tau soil}$ was observed across most of these dry regions (Fig. 7b). The ESMs sensitivity is opposite to observed for $\gamma_T^{\tau soil}$ in arid and semiarid regions. It is not clear, however, if this is induced by an inaccurate representation of soil moisture by models. In addition, most patterns of relationships between climate and τ_{soil} are similar to that between climate and τ_{eco} in Carvalhais et al. (2014), which also implies that τ_{soil} plays a dominant role in the terrestrial carbon turnover processes.

In Carvalhais et al. (2014), negative correlations were found between forest cover and τ_{eco}, suggesting that τ_{eco} does not increase with in higher forest density. Here, we performed a similar analysis for τ_{veg} and τ_{soil} in boreal forest, temperate forest, and tropical rain forest. Five

CMIP5 models were used because they output a forest cover variable. In the results (Fig. S13 in the supplemental material), we found that τ_{veg} increased with higher forest cover in the three biomes across all the five models; however, there were no consistent relationships between forest cover and τ_{soil} for most models. For observation-based results, τ_{veg} showed an increasing trend along with increased forest cover in temperate forest; τ_{veg} in boreal forest suggested an increasing trend at a threshold of 35% forest cover and then became flat beyond the threshold; and τ_{veg} did not show obvious changes with increasing forest cover in tropical rain forest. Observation-based τ_{soil} decreases with increasing forest cover in boreal forests, while there were no significant relationships between forest cover and τ_{soil} in temperate and tropical rain forest. The differences between the patterns based on observation and model mainly emerged for the relationships between forest cover and τ_{veg}. This may be because current land surface models largely simplified the real terrestrial ecosystems, while the observation-based apparent τ_{veg} reflects processes including resource competition (Stephenson et al. 2011), fire (Stephenson et al. 2011; Thonicke et al. 2001), insects (Anderegg et al. 2015), and other natural and anthropogenic disturbances (Erb et al. 2016; Fahey et al. 2005) in response to forest density. These underlying mechanisms are difficult to quantify in the present day, and require future research.

c. *Uncertainties*

It should be noted that there still exist large uncertainties in the estimation of global biomass and soil carbon turnover time. First, biomass carbon stock used in this study from Liu et al. (2015) was indirectly based on aboveground biomass (AGB) and a biome specific conversion factor from AGB to total biomass. It has been suggested that the ratios of above to belowground biomass varied with environmental conditions (Mokany et al. 2006). In addition, AGB derived with satellite-based passive microwave data in Liu et al. (2015) may saturate at a high biomass density (e.g., tropical rain forests) although it remains sensitive to biomass variations in these regions. These may contribute potential uncertainties of τ_{veg}. Here, we compared the τ_{veg} using TBC from Liu et al. (2015) and the τ_{veg} derived from the benchmark map of forest carbon stocks in tropical regions from Saatchi et al. (2011). The results suggested similar histogram patterns between the two (Fig. S14 in the supplemental material), implying that our estimates of τ_{veg} in the tropical rain forest are reliable.

Second, although efforts have been made to make global inventories of soil carbon, bias due to the interpolation of point-scale observations remains in the WISE dataset. Most current soil carbon storage data are mainly from temperate and tropical ecosystems, and more inventory data in regions such as Arctic regions are needed. We compared our global estimate of τ_{soil} with that based on soil carbon (using HWSD) and NPP from Bloom et al. (2016). The distribution of τ_{soil} (Fig. S15 in the supplemental material) was found to be similar between the two estimates.

Third, satellite-based NPP data were estimated with a radiation-based approach, through deducting the autotrophic respiration from the GPP (Zhao and Running 2010). Although this NPP observation-based product has been extensively used, including for investigating carbon turnover times (Koven et al. 2017; Thurner et al. 2016) and for benchmarking ecosystem models (Kolby Smith et al. 2016; Todd-Brown et al. 2013), it is subject to uncertainties. For example, satellite-based NPP datasets have large uncertainties in tropical regions (Cleveland et al. 2015), such as from saturation of the fraction of photosynthetically active radiation (FPAR) in high vegetation density areas, cloud and aerosol contamination, scarce meteorological data in tropical regions, and improper parameterization of the maximum light-use efficiency (LUE_{max}).

Fourth, in this study, we calculated τ_{veg} and τ_{soil} based on the steady-state assumption (input equals output), as in previous studies. This seems as an imperative choice because there is no direct measurement on the global distribution of litter fall and heterotrophic respiration. Uncertainties from the steady-state assumption are difficult to quantify from the observations in the present day, such an analysis can be conducted based on modeling output by estimating carbon turnover times from the outflux τ_{out} (Carvalhais et al. 2014). Here, outflux from biomass was calculated as in Friend et al. (2014), and outflux from soil is heterotrophic respiration. In the results, the comparisons between NPP and outflux (Figs. S16 and S17 in the supplemental material) and between carbon turnover time and τ_{out} (Figs. S18 and S19) show a strong similarity, which emphasizes the robustness of turnover time being defined from input or output under the steady-state assumption.

Fifth, when we evaluate the model-based τ_{veg} and τ_{soil} at grid scale, potential discrepancies of vegetation type and forest cover between ESMs and observation increase uncertainties. These differences limit the accuracy of the evaluation of current models for representing the spatial carbon turnover times. Because most of the CMIP5 ESMs did not report the simulated vegetation type and forest cover maps, we are still unable to evaluate the discrepancies in current time. Future model intercomparison projects are recommended to provide

these variables. Reducing these apparent influences will help us better understand and improve the internal parameterization and structure related to carbon turnover processes in current ESMs.

d. Conclusions

In summary, our results show that current ESMs underestimate biomass and soil carbon turnover times. This result implies that current ESMs may overestimate the carbon sequestration potential of biomass and soil in response to elevated atmospheric CO_2 concentration (He et al. 2016), which has been generally predicted to be the main driver of the enhancement of vegetation productivity (Zhu et al. 2016) and the terrestrial ecosystem carbon sink by ESMs (Cramer et al. 2001; Sitch et al. 2008). To reduce the large bias in the relationships between climate factors and biomass or soil carbon turnover times compared to observation, ESM developers need to calibrate the key processes affecting carbon turnover, especially in the high northern latitudes and arid and semiarid regions, so that ESMs are more closely comparable to the real world. Current limitations include the lack of representation of biotic disturbances, carbon–nutrient interactions, and permafrost–carbon climate responses. In addition, more accurate descriptions of hydrological processes and water–carbon interactions remain as a high priority for the carbon cycle modeling community.

Acknowledgments. This study was supported by the National Key R&D Program of China (2017YFA0604702), the National Natural Science Foundation of China (41530528 and 31621091), and the 111 Project (B14001).

REFERENCES

Allen, C. D., and Coauthors, 2010: A global overview of drought and heat-induced tree mortality reveals emerging climate change risks for forests. *For. Ecol. Manage.*, **259**, 660–684, https://doi.org/10.1016/j.foreco.2009.09.001.

Anav, A., and Coauthors, 2013: Evaluating the land and ocean components of the global carbon cycle in the CMIP5 Earth system models. *J. Climate*, **26**, 6801–6843, https://doi.org/10.1175/JCLI-D-12-00417.1.

Anderegg, W. R. L., and Coauthors, 2015: Tree mortality from drought, insects, and their interactions in a changing climate. *New Phytol.*, **208**, 674–683, https://doi.org/10.1111/nph.13477.

Batjes, N. H., 2016: Harmonized soil property values for broad-scale modelling (WISE30sec) with estimates of global soil carbon stocks. *Geoderma*, **269**, 61–68, https://doi.org/10.1016/j.geoderma.2016.01.034.

Bloom, A. A., and M. Williams, 2015: Constraining ecosystem carbon dynamics in a data-limited world: Integrating ecological "common sense" in a model–data fusion framework. *Biogeosciences*, **12**, 1299–1315, https://doi.org/10.5194/bg-12-1299-2015.

——, J.-F. Exbrayat, I. R. van der Velde, L. Feng, and M. Williams, 2016: The decadal state of the terrestrial carbon cycle: Global retrievals of terrestrial carbon allocation, pools, and residence times. *Proc. Natl. Acad. Sci. USA*, **113**, 1285–1290, https://doi.org/10.1073/pnas.1515160113.

Bradford, M. A., W. R. Wieder, G. B. Bonan, N. Fierer, P. A. Raymond, and T. W. Crowther, 2016: Managing uncertainty in soil carbon feedbacks to climate change. *Nat. Climate Change*, **6**, 751–758, https://doi.org/10.1038/nclimate3071.

Burke, E. J., C. D. Jones, and C. D. Koven, 2013: Estimating the permafrost-carbon climate response in the CMIP5 climate models using a simplified approach. *J. Climate*, **26**, 4897–4909, https://doi.org/10.1175/JCLI-D-12-00550.1.

Carvalhais, N., and Coauthors, 2014: Global covariation of carbon turnover times with climate in terrestrial ecosystems. *Nature*, **514**, 213–217, https://doi.org/10.1038/nature13731.

Chen, S., Y. Huang, J. Zou, and Y. Shi, 2013: Mean residence time of global topsoil organic carbon depends on temperature, precipitation and soil nitrogen. *Global Planet. Change*, **100**, 99–108, https://doi.org/10.1016/j.gloplacha.2012.10.006.

Cinquini, L., and Coauthors, 2014: The Earth System Grid Federation: An open infrastructure for access to distributed geospatial data. *Future Gener. Comput. Syst.*, **36**, 400–417, https://doi.org/10.1016/j.future.2013.07.002.

Cleveland, C. C., and Coauthors, 2015: A comparison of plot-based satellite and Earth system model estimates of tropical forest net primary production. *Global Biogeochem. Cycles*, **29**, 626–644, https://doi.org/10.1002/2014GB005022.

Corlett, R. T., 2011: Impacts of warming on tropical lowland rainforests. *Trends Ecol. Evol.*, **26**, 606–613, https://doi.org/10.1016/j.tree.2011.06.015.

Cox, P. M., D. Pearson, B. B. Booth, P. Friedlingstein, C. Huntingford, C. D. Jones, and C. M. Luke, 2013: Sensitivity of tropical carbon to climate change constrained by carbon dioxide variability. *Nature*, **494**, 341–344, https://doi.org/10.1038/nature11882.

Cramer, W., and Coauthors, 2001: Global response of terrestrial ecosystem structure and function to CO_2 and climate change: Results from six dynamic global vegetation models. *Global Change Biol.*, **7**, 357–373, https://doi.org/10.1046/j.1365-2486.2001.00383.x.

De Kauwe, M. G., and Coauthors, 2014: Where does the carbon go? A model–data intercomparison of vegetation carbon allocation and turnover processes at two temperate forest free-air CO_2 enrichment sites. *New Phytol.*, **203**, 883–899, https://doi.org/10.1111/nph.12847.

Doughty, C. E., and M. L. Goulden, 2008: Are tropical forests near a high temperature threshold? *J. Geophys. Res.*, **113**, G00B07, https://doi.org/10.1029/2007JG000632.

Erb, K.-H., and Coauthors, 2016: Biomass turnover time in terrestrial ecosystems halved by land use. *Nat. Geosci.*, **9**, 674–678, https://doi.org/10.1038/ngeo2782.

Fahey, T. J., and Coauthors, 2005: The biogeochemistry of carbon at Hubbard Brook. *Biogeochemistry*, **75**, 109–176, https://doi.org/10.1007/s10533-004-6321-y.

FAO/IIASA/ISRIC/ISSCAS/JRC, 2012: Harmonized World Soil Database (version 1.2). Food and Agriculture Organization of the United Nations (FAO) and International Institute for Applied Systems Analysis (IIASA), http://www.fao.org/soils-portal/soil-survey/soil-maps-and-databases/harmonized-world-soil-database-v12/en/.

Flato, G., and Coauthors, 2013: Evaluation of climate models. *Climate Change 2013: The Physical Science Basis*, T. F. Stocker et al., Eds., Cambridge University Press, 741–866.

Forkel, M., N. Carvalhais, C. Rödenbeck, R. Keeling, M. Heimann, K. Thonicke, S. Zaehle, and M. Reichstein, 2016: Enhanced seasonal CO_2 exchange caused by amplified plant productivity in northern ecosystems. *Science*, **351**, 696–699, https://doi.org/10.1126/science.aac4971.

Franklin, J. F., H. Shugart, and M. E. Harmon, 1987: Tree death as an ecological process. *BioScience*, **37**, 550–556, https://doi.org/10.2307/1310665.

Friedl, M. A., D. Sulla-Menashe, B. Tan, A. Schneider, N. Ramankutty, A. Sibley, and X. Huang, 2010: MODIS Collection 5 global land cover: Algorithm refinements and characterization of new datasets. *Remote Sens. Environ.*, **114**, 168–182, https://doi.org/10.1016/j.rse.2009.08.016.

Friedlingstein, P., and Coauthors, 2006: Climate–carbon cycle feedback analysis: Results from the C^4MIP model intercomparison. *J. Climate*, **19**, 3337–3353, https://doi.org/10.1175/JCLI3800.1.

——, M. Meinshausen, V. K. Arora, C. D. Jones, A. Anav, S. K. Liddicoat, and R. Knutti, 2014: Uncertainties in CMIP5 climate projections due to carbon cycle feedbacks. *J. Climate*, **27**, 511–526, https://doi.org/10.1175/JCLI-D-12-00579.1.

Friend, A. D., and Coauthors, 2014: Carbon residence time dominates uncertainty in terrestrial vegetation responses to future climate and atmospheric CO_2. *Proc. Natl. Acad. Sci. USA*, **111**, 3280–3285, https://doi.org/10.1073/pnas.1222477110.

Gibbs, H. K., L. Olsen, and T. Boden, 2006: Major world ecosystem complexes ranked by carbon in live vegetation: An updated database using the GLC2000 land cover product. Oak Ridge National Laboratory, https://doi.org/10.3334/CDIAC/lue.ndp017.2006.

Greaver, T. L., and Coauthors, 2016: Key ecological responses to nitrogen are altered by climate change. *Nat. Climate Change*, **6**, 836–843, https://doi.org/10.1038/nclimate3088.

Harris, I., P. Jones, T. Osborn, and D. Lister, 2014: Updated high-resolution grids of monthly climatic observations—The CRU TS3.10 dataset. *Int. J. Climatol.*, **34**, 623–642, https://doi.org/10.1002/joc.3711.

He, Y., S. E. Trumbore, M. S. Torn, J. W. Harden, L. J. S. Vaughn, S. D. Allison, and J. T. Randerson, 2016: Radiocarbon constraints imply reduced carbon uptake by soils during the 21st century. *Science*, **353**, 1419–1424, https://doi.org/10.1126/science.aad4273.

Hugelius, G., C. Tarnocai, G. Broll, J. Canadell, P. Kuhry, and D. Swanson, 2013: The Northern Circumpolar Soil Carbon Database: Spatially distributed datasets of soil coverage and soil carbon storage in the northern permafrost regions. *Earth Syst. Sci. Data*, **5**, 3–13, https://doi.org/10.5194/essd-5-3-2013.

Janssens, I. A., and Coauthors, 2010: Reduction of forest soil respiration in response to nitrogen deposition. *Nat. Geosci.*, **3**, 315–322, https://doi.org/10.1038/ngeo844.

Jiang, L., and Coauthors, 2015: Scale-dependent performance of CMIP5 Earth system models in simulating terrestrial vegetation carbon. *J. Climate*, **28**, 5217–5232, https://doi.org/10.1175/JCLI-D-14-00270.1.

Jones, P. W., 1999: First- and second-order conservative remapping schemes for grids in spherical coordinates. *Mon. Wea. Rev.*, **127**, 2204–2210, https://doi.org/10.1175/1520-0493(1999)127<2204:FASOCR>2.0.CO;2.

Knorr, W., I. C. Prentice, J. I. House, and E. A. Holland, 2005: Long-term sensitivity of soil carbon turnover to warming. *Nature*, **433**, 298–301, https://doi.org/10.1038/nature03226.

Kolby Smith, W., S. C. Reed, C. C. Cleveland, A. P. Ballantyne, W. R. L. Anderegg, W. R. Wieder, Y. Y. Liu, and S. W. Running, 2016: Large divergence of satellite and Earth system model estimates of global terrestrial CO_2 fertilization. *Nat. Climate Change*, **6**, 306–310, https://doi.org/10.1038/nclimate2879.

Koven, C. D., B. Ringeval, P. Friedlingstein, P. Ciais, P. Cadule, D. Khvorostyanov, G. Krinner, and C. Tarnocai, 2011: Permafrost carbon–climate feedbacks accelerate global warming. *Proc. Natl. Acad. Sci. USA*, **108**, 14 769–14 774, https://doi.org/10.1073/pnas.1103910108.

——, and Coauthors, 2015: Controls on terrestrial carbon feedbacks by productivity vs. turnover in the CMIP5 Earth system models. *Biogeosciences*, **12**, 5211–5228, https://doi.org/10.5194/bgd-12-5757-2015.

——, G. Hugelius, D. M. Lawrence, and W. R. Wieder, 2017: Higher climatological temperature sensitivity of soil carbon in cold than warm climates. *Nat. Climate Change*, **7**, 817–822, https://doi.org/10.1038/nclimate3421.

Le Quéré, C., and Coauthors, 2015: Global carbon budget 2015. *Earth Syst. Sci. Data*, **7**, 349–396, https://doi.org/10.5194/essd-7-349-2015.

Liu, Y. Y., R. A. M. de Jeu, M. F. McCabe, J. P. Evans, and A. I. J. M. van Dijk, 2011: Global long-term passive microwave satellite-based retrievals of vegetation optical depth. *Geophys. Res. Lett.*, **38**, L18402, https://doi.org/10.1029/2011GL048684.

——, A. I. J. M. van Dijk, R. A. M. de Jeu, J. G. Canadell, M. F. McCabe, J. P. Evans, and G. Wang, 2015: Recent reversal in loss of global terrestrial biomass. *Nat. Climate Change*, **5**, 470–474, https://doi.org/10.1038/nclimate2581.

Melillo, J. M., and Coauthors, 2002: Soil warming and carbon-cycle feedbacks to the climate system. *Science*, **298**, 2173–2176, https://doi.org/10.1126/science.1074153.

Mitchell, T. D., and P. D. Jones, 2005: An improved method of constructing a database of monthly climate observations and associated high-resolution grids. *Int. J. Climatol.*, **25**, 693–712, https://doi.org/10.1002/joc.1181.

Mokany, K., R. Raison, and A. S. Prokushkin, 2006: Critical analysis of "root : shoot" ratios in terrestrial biomes. *Global Change Biol.*, **12**, 84–96, https://doi.org/10.1111/j.1365-2486.2005.001043.x.

Nemani, R. R., C. D. Keeling, H. Hashimoto, W. M. Jolly, S. C. Piper, C. J. Tucker, R. B. Myneni, S. W. Running, 2003: Climate-driven increases in global terrestrial net primary production from 1982 to 1999. *Science*, **300**, 1560–1563, https://doi.org/10.1126/science.1082750.

New, M., M. Hulme, and P. Jones, 2000: Representing twentieth-century space–time climate variability. Part II: Development of 1901–96 monthly grids of terrestrial surface climate. *J. Climate*, **13**, 2217–2238, https://doi.org/10.1175/1520-0442(2000)013<2217:RTCSTC>2.0.CO;2.

Niu, S., M. Wu, Y. I. Han, J. Xia, Z. H. E. Zhang, H. Yang, and S. Wan, 2010: Nitrogen effects on net ecosystem carbon exchange in a temperate steppe. *Global Change Biol.*, **16**, 144–155, https://doi.org/10.1111/j.1365-2486.2009.01894.x.

Peylin, P., and Coauthors, 2005: Multiple constraints on regional CO_2 flux variations over land and oceans. *Global Biogeochem. Cycles*, **19**, 1–21, https://doi.org/10.1029/2003GB002214.

Piao, S., and Coauthors, 2013: Evaluation of terrestrial carbon cycle models for their response to climate variability and to CO_2 trends. *Global Change Biol.*, **19**, 2117–2132, https://doi.org/10.1111/gcb.12187.

Raffa, K. F., B. H. Aukema, B. J. Bentz, A. L. Carroll, J. A. Hicke, M. G. Turner, and W. H. Romme, 2008: Cross-scale drivers of natural disturbances prone to anthropogenic amplification: The dynamics of bark beetle eruptions. *BioScience*, **58**, 501–517, https://doi.org/10.1641/B580607.

Robinson, D., 2007: Implications of a large global root biomass for carbon sink estimates and for soil carbon dynamics. *Proc. Biol. Sci.*, **274**, 2753–2759, https://doi.org/10.1098/rspb.2007.1012.

Saatchi, S. S., and Coauthors, 2011: Benchmark map of forest carbon stocks in tropical regions across three continents. *Proc. Natl. Acad. Sci. USA*, **108**, 9899–9904, https://doi.org/10.1073/pnas.1019576108.

Schuur, E. A. G., and Coauthors, 2015: Climate change and the permafrost carbon feedback. *Nature*, **520**, 171–179, https://doi.org/10.1038/nature14338.

Sitch, S., and Coauthors, 2008: Evaluation of the terrestrial carbon cycle, future plant geography and climate-carbon cycle feedbacks using five dynamic global vegetation models (DGVMs). *Global Change Biol.*, **14**, 2015–2039, https://doi.org/10.1111/j.1365-2486.2008.01626.x.

Stephenson, N. L., P. J. van Mantgem, A. G. Bunn, H. Bruner, M. E. Harmon, K. B. O'Connell, D. L. Urban, and J. F. Franklin, 2011: Causes and implications of the correlation between forest productivity and tree mortality rates. *Ecol. Monogr.*, **81**, 527–555, https://doi.org/10.1890/10-1077.1.

Tarnocai, C., J. Canadell, E. Schuur, P. Kuhry, G. Mazhitova, and S. Zimov, 2009: Soil organic carbon pools in the northern circumpolar permafrost region. *Global Biogeochem. Cycles*, **23**, GB2023, https://doi.org/10.1029/2008GB003327.

Taylor, K. E., R. J. Stouffer, and G. A. Meehl, 2012: An overview of CMIP5 and the experiment design. *Bull. Amer. Meteor. Soc.*, **93**, 485–498, https://doi.org/10.1175/BAMS-D-11-00094.1.

Thonicke, K., S. Venevsky, S. Sitch, and W. Cramer, 2001: The role of fire disturbance for global vegetation dynamics: Coupling fire into a dynamic global vegetation model. *Global Ecol. Biogeogr.*, **10**, 661–677, https://doi.org/10.1046/j.1466-822X.2001.00175.x.

Thurner, M., C. Beer, N. Carvalhais, M. Forkel, M. Santoro, M. Tum, and C. Schmullius, 2016: Large-scale variation in boreal and temperate forest carbon turnover rate related to climate. *Geophys. Res. Lett.*, **43**, 4576–4585, https://doi.org/10.1002/2016GL068794.

——, and Coauthors, 2017: Evaluation of climate-related carbon turnover processes in global vegetation models for boreal and temperate forests. *Global Change Biol.*, **23**, 3076–3091, https://doi.org/10.1111/gcb.13660.

Tian, H., and Coauthors, 2015: Global patterns and controls of soil organic carbon dynamics as simulated by multiple terrestrial biosphere models: Current status and future directions. *Global Biogeochem. Cycles*, **29**, 775–792, https://doi.org/10.1002/2014GB005021.

Todd-Brown, K., J. Randerson, W. Post, F. Hoffman, C. Tarnocai, E. Schuur, and S. Allison, 2013: Causes of variation in soil carbon simulations from CMIP5 Earth system models and comparison with observations. *Biogeosciences*, **10**, 1717–1736, https://doi.org/10.5194/bg-10-1717-2013.

——, and Coauthors, 2014: Changes in soil organic carbon storage predicted by Earth system models during the 21st century. *Biogeosciences*, **11**, 2341–2356, https://doi.org/10.5194/bg-11-2341-2014.

Tribuzy, E. S., 2005: Variações da temperatura foliar do dossel e o seu efeito na taxa assimilatória de CO_2 na Amazônia Central. Ph.D. thesis, Universidade de São Paulo, 102 pp., https://doi.org/10.11606/T.91.2005.tde-15072005-144011.

Van Mantgem, P. J., and N. L. Stephenson, 2007: Apparent climatically induced increase of tree mortality rates in a temperate forest. *Ecol. Lett.*, **10**, 909–916, https://doi.org/10.1111/j.1461-0248.2007.01080.x.

Wang, X., and Coauthors, 2014: Soil respiration under climate warming: Differential response of heterotrophic and autotrophic respiration. *Global Change Biol.*, **20**, 3229–3237, https://doi.org/10.1111/gcb.12620.

Wang, X., and Coauthors, 2014: A two-fold increase of carbon cycle sensitivity to tropical temperature variations. *Nature*, **506**, 212–215, https://doi.org/10.1038/nature12915.

Wieder, W. R., M. D. Hartman, B. Sulman, Y.-P. Wang, C. D. Koven, and G. B. Bonan, 2018: Carbon cycle confidence and uncertainty: Exploring variation among soil biogeochemical models. *Global Change Biol.*, **24**, 1563–1579, https://doi.org/10.1111/gcb.13979.

Williams, A. P., C. D. Allen, C. I. Millar, T. W. Swetnam, J. Michaelsen, C. J. Still, and S. W. Leavitt, 2010: Forest responses to increasing aridity and warmth in the southwestern United States. *Proc. Natl. Acad. Sci. USA*, **107**, 21 289–21 294, https://doi.org/10.1073/pnas.0914211107.

——, and Coauthors, 2013: Temperature as a potent driver of regional forest drought stress and tree mortality. *Nat. Climate Change*, **3**, 292–297, https://doi.org/10.1038/nclimate1693.

Zhao, M., and S. W. Running, 2010: Drought-induced reduction in global terrestrial net primary production from 2000 through 2009. *Science*, **329**, 940–943, https://doi.org/10.1126/science.1192666.

——, F. A. Heinsch, R. R. Nemani, and S. W. Running, 2005: Improvements of the MODIS terrestrial gross and net primary production global data set. *Remote Sens. Environ.*, **95**, 164–176, https://doi.org/10.1016/j.rse.2004.12.011.

Zhu, Z., and Coauthors, 2016: Greening of the Earth and its drivers. *Nat. Climate Change*, **6**, 791–795, https://doi.org/10.1038/nclimate3004.